Engineering Structures 280 (2023) 115696

Contents lists available at ScienceDirect

Engineering Structures

journal homepage: www.elsevier.com/locate/engstruct

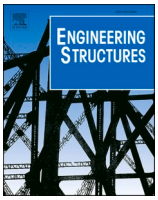

Light timber framed wall under fire: Effect of the load and cladding

Paulo A.G. Piloto [a,*], Diego Vergara [b]

[a] Instituto Politécnico de Bragança, Campus de Santa Apolónia, 5300-253 Bragança, Portugal
[b] Department of Mechanical Engineering, Catholic University of Ávila, C/Canteros, s/n, 05005 Avila, Spain

ARTICLE INFO

Keywords:
Fire
Walls
Gypsum
Load-bearing
Experimental tests
Modelling

ABSTRACT

Light Timber Frame Walls are made of solid timber elements and are usually protected by cladding materials (gypsum). This investigation finds the effect of different load levels and cladding systems on the fire resistance. The timber frame structure is made with three studs and two rails, and will be analysed with two different protection levels. The computational model includes the thermal analysis under standard fire and a sequential mechanical analysis with time increments. Both, thermal and thermo-mechanical models are validated against experimental results developed in the reduced scale and full scale. The timber frame structure is deemed to have failed when it is no longer supporting the test load. The results are also compared with the failure criteria used for the experimental tests. The timber frame is deformed and all simulated models attained the global bucking instability mode, with studs moving to the outside of the furnace, due to the effect of load and charred layer. The fire resistance of a double-layered light timber frame wall is higher than a single-layered, and both decrease with the load level. This ability is reduced by 46%, on average for all load levels, when using only one gypsum layer. A new formula is proposed to determine the fire resistance, based on the load level and cladding systems. The fire resistance of the specimens with two layers of gypsum plates decreases faster than the specimens with one layer of gypsum, with respect to the increase of the load level.

1. Introduction

Lightweight Timber Framed Walls (LTFW) are commonly used in residential, industrial and commercial buildings due to their lightweight and low construction costs. LTFW are made with solid wood members (studs and rails) used on buildings, for load-bearing and partition walls. The assemblies are made with solid stud wood vertical members, usually separated by 400–600 mm. The cladding for internal walls may be developed with wood panels, composite panels and or gypsum panels. The number of protection layers and insulation materials used in the cavity of the wall depends on the thermal and acoustic efficiency required for the LTFW at room temperature, but also depends on the required fire rating of LTFW.

Designers should reduce the fire risk of timber buildings, limiting the spread of the flames and hot gases, allowing the inhabitants to escape, thereby protecting their lives, and allowing the fire brigades to do their job safely. Building fire documents should include the fire safety class of the materials and the fire resistance of the elements. These last ones should comply with the fire requirements for the compartment. Structural elements, cladding and surface finish, depending on their assigned functionality, are required to have the ability to sustain the load without separating functions complying with their fire rating (from R15 to R360), or are required to have the partitioning ability to avoid the passage of flames and hot gases complying with their fire rating (from RE20 to RE360), or the partitioning ability to sustain the temperature in the unexposed side (from REI 15 to REI360) [1]. Requirements for these attributes depend on the building type, and particularly on the building height (REI60 may be required for a timber building with four stories, while REI90 may be required for higher buildings).

Building elements under fire may be designed using simplified rules or advanced calculation methods [2]. In any case, the fire design starts by finding the load combination and then by finding the reduction of the cross section due to the combustion effect. The reduction of the cross section depends on the fire rating specified and on the charring rate of the timber element. After all, designers need to check if the stud or the rail can sustain the load with the residual cross section expected. When considering the LTFW, the cross section of the solid elements is usually a small value (45 mm on the shortest side) and, for that reason, a cladding system is required to achieve the required fire rating.

During the last few years, some experimental tests have been carried

* Corresponding author.
E-mail addresses: ppiloto@ipb.pt (P.A.G. Piloto), diego.vergara@ucavila.es (D. Vergara).

https://doi.org/10.1016/j.engstruct.2023.115696
Received 7 September 2022; Received in revised form 6 January 2023; Accepted 22 January 2023

out. In 1994, Mehaffey et al. [3] developed some experimental tests to validate the 2D numerical model. In 1995, Thomas et al. [4] developed a parametric numerical study to find the time when charring of the timber would first occur, and the time at which an insulation failure would occur. One year later, in 1996, Thomas [5] presented one experimental real fire test developed in one room compartment and compare the wall temperature results with the 2D finite element model, using TASEF. The numerical results improved when using the bulk temperature measured from the experimental test. Later in 1998, Takeda and Mehaffey [6] used the same experimental tests to improve the 2D model, enhancing the description of heat transfer through the entire assembly, in particular across the cavity region. These experimental tests were already used for the validation of the 2D numerical model using Ansys, developed recently by Piloto and Fonseca [7]. Scott Young in 2000 [8] developed an extensive experimental investigation regarding LTF wall panels at room temperature and under fire conditions in order to determine the time to failure, the failure modes and the effect of restraints on the performance of load-bearing walls. A simplified 3D numerical model including a single stud was developed, predicting displacements with accuracy. In 2001, Clancy [9] reviewed the progress made in modelling heat transfer through LTF structures exposed to fire, presenting also some experimental results. The model included the implicit motion of moisture and vapour, the modelling of re-entrant corners in void cavities, and the ablation of the gypsum layers. In the same year, Young and Clancy [10] developed a structural model to determine the behaviour of LTFW based on a single stud under fire, following performance-based building regulations. According to these authors, this closed-form model is accurate. Gypsum boards are also contributing to the initial structural fire resistance of the LTFW, when working in tension and when exposed to low temperatures (below 100 °C). In 2002, Collier and Buchanan [11] developed a numerical model using finite differences, to predict the fire resistance of non load-bearing or load-bearing LTFW when exposed to realistic and standard fire. For the heat transfer across the void cavity, both radiation and convection modes of heat transfer were used, which is in line with the current investigation. According to these authors, studs are modelled as axially loaded columns and the fire effect is predicted by the residual cross-section in the studs and the calculation of the residual load-bearing capacity. Their model does not consider the effect of the timber frame (assembly) and the effect of other efforts developed during the fire. In 2002, Clancy [12] developed a parametric analysis to predict the structural time-to-failure of gypsum cladding LTFW under fire. The study found that the most dominant variables, by order of importance are the depth and the width of studs, the fire scenario, the thickness of the gypsum layer, the elastic modulus of wood in compression, the enthalpy of gypsum and the load applied. These authors concluded that load is not as dominant as could be expected. In 2010, Thomas [13] evaluated the thermal performance analysis, using the finite element code SAFIR and TASEF, concerning the temperature results obtained from several experimental tests, analysing the contribution by the gypsum material. This author concluded that both softwares present good results for slower developing fires and furnace tests when compared with rapidly growing fires. Thomas [13] also concluded that the best thermal properties of gypsum material should include the effect of two dehydration reactions and a third calcination reaction. More recently, in 2021, Frank Kang [14] developed three experimental tests for load-bearing LTFW evaluation, submitted to fire from both sides. These tests consisted of two different thicknesses of gypsum plasterboard, two different load levels, and two widths of wall opening at each end of the load-bearing wall specimen to enhance the equality of the fire scenario from both sides. This investigation was complemented by a 2D computational model for thermal analysis and by a 3D model based on a single stud, assuming the same temperature field from the bottom stud up to the top. Both thermal and mechanical models have been validated against experimental results, with permission from Winstone Wallboards Ltd. A parametric analysis has been developed considering different stud geometries, different gypsum thicknesses, different load levels, and different fire scenarios (one side and two sides exposed). In 2022, Piloto et al. [15] developed a parametric analysis using a 2D model to demonstrate the effect of the depth and distance between studs on the fire resistance (insulation), while these parameters are not included in the separating function method presented in the next generation of the prEN1995-1-2 [2]. More recently, Piloto et al [16] developed a numerical investigation regarding the fire rating of load-bearing LTFW, including the comparison of the charring layer over time with the current and future version of Eurocode 5, part 1.2.

This current investigation presents a fully assembled LTFW, using a 3D finite element model. This model was validated for temperatures in a reduced scale for non load-bearing specimens, developed by the authors, and also validated for temperature and displacements with a full scale model for load-bearing specimen, developed by Frank Kang [14]. A parametric analysis is also presented to find the fire resistance of a LTFW using different load levels and cladding systems. A new proposal is presented for reduced scale specimens, with a correlation between time to failure and the load level, from 5 to 20%. The load level is defined by the percentage of the load-bearing determine at room temperature.

2. Methodology

This numerical investigation finds the time to structural failure of one timber frame (reduced scale), made with softwood solid timber, protected by one and two gypsum layers. It is assumed that gypsum does not contribute to the load-bearing of the timber frame. This LTFW model is assumed to be positioned inside a rigid frame with the bottom end fixed to the frame. The load is applied on top and both lateral edges are free to move down, move out of the plane of the frame and they are restrained to move in-plane towards the frame direction due to the lateral gaps between the specimen and the frame. The external studs are free to move in-plane towards the direction of the central stud.

The numerical simulations are based on four solution methods (elastic buckling analysis to find the critical load and mode of instability, which can help to introduce the global imperfection of the timber frame, Geometric and Material Non Linear Imperfection Analysis (GMNIA) to find the load-bearing at room temperature, the non linear transient thermal analysis to find the temperature of the materials involved in the fire simulations (frame and cladding system), and finally, the GMNIA to find the time to the structural failure using a thermo-mechanical analysis).

The elastic buckling analysis was developed to find the critical load and mode of instability. The block Lanczos extraction method [17] has been used to this end. The first instability mode has been used to define the geometric imperfection of the timber frame, for both the reduced scale model and the full-scale model.

The GMNIA used to find the load-bearing capacity of the timber frame was developed with an incremental load procedure. This maximum load has been determined using the arc-length method [18].

The thermal analysis usually considers the effect of the standard fire only from one exposed side, which has been the case for the reduced scale model. During the validation of the numerical models, different fire scenarios have been used. For the reduced scale model case, the standard fire ISO834 has been applied for the bulk temperature of the exposed side, assuming to keep 20 °C in the bulk temperature of the unexposed side. For the validation of the full-scale model, and because this load-bearing model considers the wall submitted to fire from both sides, the standard fire ISO834 has been applied for the bulk temperature of the furnace side, while a different fire scenario (lower bulk temperature) has been applied on the other side (due to the limitation of the experimental testing facilities). Two numerical techniques have been used, based on our previous experience to validate 3D numerical models [19,20]. For the reduced-scale model, an extra boundary condition for convection and radiation is considered inside the cavity, based on the bulk cavity temperature measured during the experimental tests developed in the LTFW with a single and a double cladding system. This extra

boundary condition can predict any material degradation of the cladding system and the effect of the combustion process of the timber frame. For the full-scale model, and because there was no cavity temperature measured during the experiments, only radiation has been considered, using an interface surface element to determine the bulk temperature of the cavity. The solution method is considered incremental and iterative, due to the non-linearities involved in the material properties and boundary conditions. The time step was selected to be 60 (s), but can be reduced to 1 (s). The criterion used for convergence of the solution is based on the heat flow, using a tolerance value of 0.1% and a reference value of 10^{-6} W. Based on previous numerical research [20], one additional boundary condition is applied to all the internal surfaces of the cavity. The convection coefficient is set to be $\alpha_c = 17$ (W/m^{2}K) and the emissivity of the flames is $\varepsilon_f = 1.0$, assuming that the bulk temperature of the cavity is following the standard fire test condition. The convection coefficient is an average value between the exposed and unexposed sides of the fire exposed LTFW [21]. This value may be justified by the fact that the cavity is not directly exposed to fire during all testing time and depends on the gypsum cracking and ablation. The cavity region is not exposed in the beginning, is partially exposed during the test and is fully exposed at the end of the test.

The structural analysis under fire is developed using the Newton Raphson method [22], considering an incremental solution based on a time step of 60 s, with the possibility to be reduced to 0.001 s. The iterative solution is based on a tolerance criterion of 0.001 in force and moment, using a reference value of 1 N and 1Nm.

The experimental investigation considered the international standards for testing. For the case of non load-bearing walls, the fire resistance should be verified for the insulation (I) and integrity (E), usually using the procedures defined in EN1363-1 [23], EN1364-1 [24], ISO834 [25]. The two experimental tests have been developed for the reduced scale model, at the Polytechnic Institute of Bragança (IPB), in Portugal.

In the case of the load-bearing wall, the vertical load is transmitted through the studs and the cladding system may increase the stability of the wall, depending on the stiffness of the connection between the panels and the studs. The fire resistance should be verified for the load-bearing capacity (R), insulation (I) and integrity (E), usually using experimental standard tests, where specimen instrumentation and criteria are defined on AS 1530.4 [26]. The experimental test under consideration has been developed by Frank Kang [14] and the test has been conducted in a vertical furnace at the fire testing laboratory of the Building Research Association in New Zealand (BRANZ). The fire-resistance wall test method defined in AS 1530.4 does not consider two-sided fire exposure, bringing a new challenge to the fire behaviour of LTFW exposure to both sides of the specimen. The fire-resistance test QR1810-162 has been selected and more details will be presented herein.

The insulation criterion (I) measures the ability of the element to keep the unexposed side below a certain temperature level, tracking the average and maximum temperatures, and avoiding the ignition of the materials in the adjacent compartment and fire spread. The criteria define the time, in completed minutes, for which the test specimen continues to maintain its separating function during the test without developing temperatures on its unexposed surface which increase the average temperature above the initial average temperature by more than 140 K, or increase the temperature, at any location, above the initial average temperature by more than 180 K. The loadbearing criterion (R) measures the ability of the slab to support the imposed load. The criterion is determined from the measurements of the maximum deflection (C) or the rate of deflection (dC/dt), following the definitions presented in Table 1, where h represents the initial height of the test specimen, once the load is applied.

Load-bearing and partition wall systems used in residential and commercial properties in Europe are required to provide fire rating according to standard EN13501-2 [1], used for the fire classification of construction products and building elements. Partition walls can be rated for EI, from 15 to 240 min, while the load-bearing elements can be rated for REI, from 15 to 360 min. The safety level is then selected by European countries, using their national level safety system.

Table 1
Fire resistance criterion for load-bearing (R).

Criterion	Formula	unity
C_{lim}	$h/100$	(mm)
$(dC/dt)_{lim}$	$3h/1000$	(mm/min)

3. Reduced, full-scale models and materials

The reduced scale LTFW assemblies are made with softwood Douglas fir, using 3 solid timber elements for studs and 2 solid timber elements for rails, each using a cross section of 100 × 50 mm. The dimensions are defined according to the IPB furnace testing dimensions, see Fig. 1. This geometry has been used, also, for the parametric study.

The geometry used for the validation of the full-scale model was also adjusted to the BRANZ laboratory facilities, considering that the specimen has been submitted no fire from both sides, when using a vertical furnace with dimensions of 3 m wide and 4 m high. The LTFW specimen QR1810-16 consisted of 5 load-bearing timber studs with 90 × 45 mm, spaced every 400 mm, with extra 2 non load-bearing studs, positioned 177.5 mm away and with 100 mm gap at mid-height. This timber frame has been protected on both sides and lateral extremities by gypsum plates with 16 mm with 925 kg/m^3 density. The specimen used two rows of timber nogs spaced every 1 m, see Fig. 2.

The reduced scale model has been exposed to fire from one side and the model is represented in Fig. 3, while the full-scale model has been exposed to fire from both sides and the model is depicted in Fig. 4.

The material properties involved are the thermal properties of wood and gypsum (conductivity, specific heat, density and emissivity) and the mechanical properties of wood members (orthotropic elastic, plastic, and damage criterion). Gypsum is not considered for load-bearing even with the existence of self-screwing bolts.

The thermal properties of both materials used in the parametric analysis are presented in Fig. 5 and they are based on softwood Douglas fir with a density of 722 kg/m^3 and very low moisture content, based on the EN1995-1.2 [27] and gypsum used by Sultan [28] with 698 kg/m^3, respectively. The emissivity used for both materials is 0.8. The thermal behaviour of gypsum considers only two main reactions when exposed to elevated temperatures. The thermal properties used in the validation of the reduced scale model changed according to the company specifications and the location of the experiments, see Fig. 5. The reduced-scale model considers softwood Douglas fir with the same characteristics, while the full-scale model considers SG8 Radiata Pine with 12% moisture and an average value for the density of 510 kg/m^3. The gypsum follows the material property evolution of the gypsum plasterboard defined in prEN1995-1-2 [2], using gypsum plates of 12.5 mm thickness and density equal to 698 kg/m^3. The thermal properties used in the validation of the full-scale model are based on the work developed by Frank Kang [14], see Fig. 5, with a modification regarding the specific heat [2]. This modification removes two inflexions in the numerical results obtained for the temperature evolution between 100 and 220 °C that were not registered in the experimental results. The thermal conductivity and density are based on the thermal properties defined by Frank Kang [14], using the data from Thomas [5].

The mechanical properties are only presented for the material that is capable to bear the vertical load. Wood is a highly anisotropic material, due to the way the tree grows and the arrangement of the wood cells within the stem. Wood can be considered locally as an orthotropic material that includes three principal directions. The wood model considers different behaviour of the material in the direction of the fibres, radial direction, and tangential direction. The strength and stiffness of wood are considerably higher in the longitudinal than in the other orthogonal

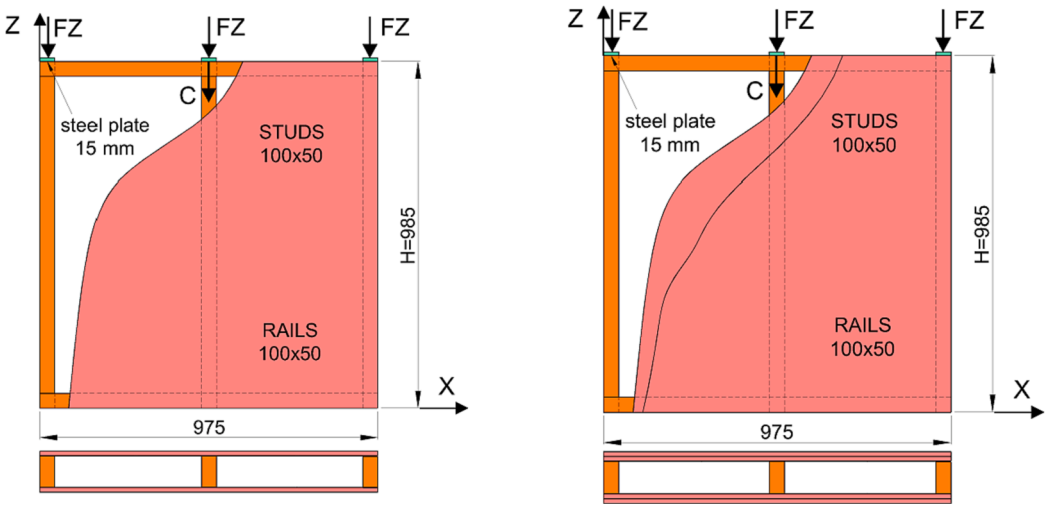

Fig. 1. Reduced scale LTFW with one and two gypsum layers.

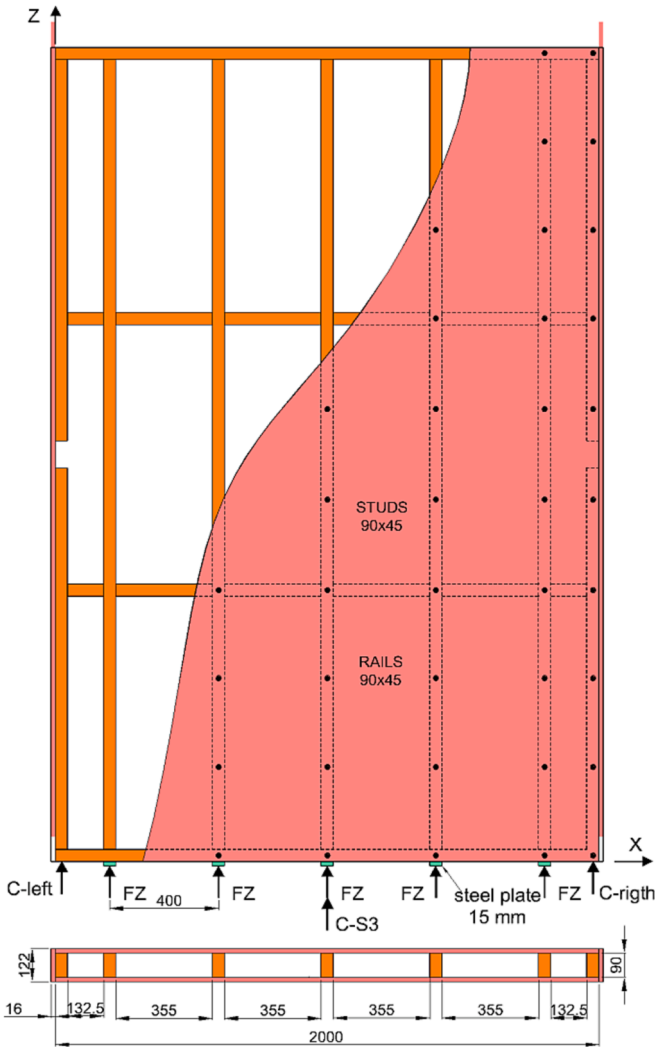

Fig. 2. Full-scale LTFW protected by one gypsum layer.

directions. This can be easily understood based on the percentage of the fibres being longitudinally oriented [29]. The generalized Hooke law for an orthotropic material is considered. Table 2 gives the values used for

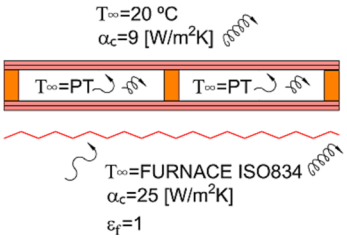

Fig. 3. Thermal boundary conditions for the reduced scale model.

the elastic behaviour of the material. This material model considers the reduction coefficient for elevated temperatures, assuming 5% of the room temperature values for residual strength and stiffness at 300 °C and for temperatures above. Moreover, According to EN1995-1-2 [27], it is possible to conclude that the strength of wood in the direction parallel to the grain (direction x) is linearly reduced with increasing temperature, more accentuated up to 100 (°C). The modulus of elasticity (E_X, E_Y, E_Z) is also affected by the increase in temperature, applying the reduction factors between 100 and 300 (°C). Poisson's coefficients (ν_{XY}, ν_{YZ},ν_{XZ}) are considered constant in the face of temperature rise, because the current version of the EN1995-1-2 [15] and the next generation [2] do not define correction factors to be applied for this property.

The transverse elastic modulus (G_{XY}, G_{YZ}, G_{XZ}) also undergoes a reduction with increasing temperature, and the same reduction coefficients of the modulus of elasticity are being used, since both elastic properties of wood are related through Poisson's coefficients. The failure of wood can be presented in several ways, such as fibre breakage, microcracking of the matrix, detachment of fibres or delamination. To characterize this effect, the Hill criterion is adopted [30]. This criterion is based on von Mises's theory and adapted for orthotropic materials. Hill's criterion considers the interaction between the stress in the failure mechanism and depends on the orientation of the stress concerning the orthotropic axis of the material. This criterion allows the determination of the elastic and elastoplastic zones in the stress–strain relationship of the wood. The characteristic parameters of the orthotropic material, defined for this criterion, are the R_{ij} yield rates, which are established as a function of the limit stress in the main directions of the material. Assuming that the wood does not have the plastic capacity, the elastic perfectly plastic regime is considered for the constitutive law in this investigation just to ensure that the material has an elastic limit. The tensile strength f_{xx}^{y} value was determined by experimental measurements at room temperature and considered to be 44.49, 28.92 and 0.44 (MPa), for each temperature level (20, 100 and 300 (°C)) [31]. Table 3

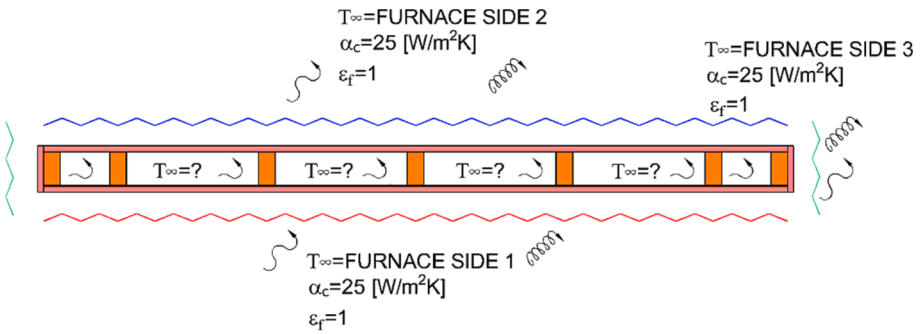

Fig. 4. Thermal boundary conditions for the full-scale model.

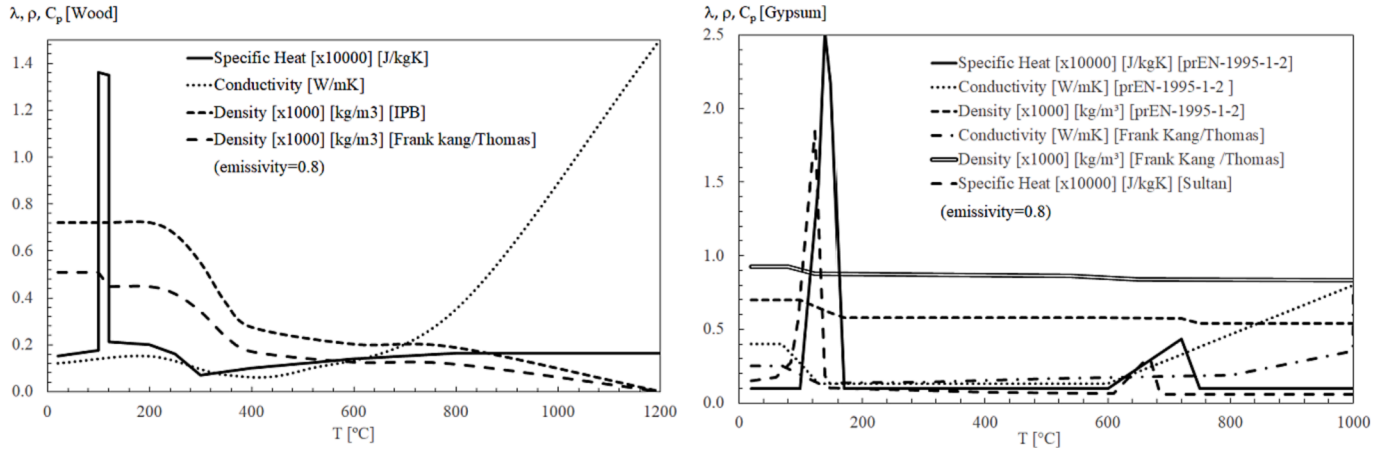

Fig. 5. Thermal properties used for timber and gypsum.

Table 2
Linear elastic orthotropic properties for softwood Douglas fir [27].

	20 (°C)	100 (°C)	300 (°C)
E_X (Pa)	11.20×10^9	5.600×10^9	0.112×10^9
E_Y (Pa)	0.448×10^9	0.224×10^9	0.004×10^9
E_Z (Pa)	0.985×10^9	0.493×10^9	0.009×10^9
ν_{XY}	0.315	0.315	0.315
ν_{YZ}	0.308	0.308	0.308
ν_{XZ}	0.347	0.347	0.347
G_{XY} (Pa)	0.907×10^9	0.454×10^9	0.009×10^9
G_{YZ} (Pa)	0.123×10^9	0.061×10^9	0.001×10^9
G_{XZ} (Pa)	1.075×10^9	0.538×10^9	0.010×10^9

Table 3
Strength limit in tension and Hill coefficients for softwood Douglas fir [31].

	20 (°C)	100 (°C)	300 (°C)
f^y(Pa)	44.90×10^6	28.92×10^6	0.449×10^6
$R_{XX}=f^y_{xx}/f^y$	1	1	1
$R_{YY}=f^y_{yy}/f^y$	0.052	0.052	0.052
$R_{ZZ}=f^y_{zz}/f^y$	0.052	0.052	0.052
$R_{XY}=f^y_{xy}/(f^y/\sqrt{3})$	0.405	0.405	0.179
$R_{YZ}=f^y_{yz}/(f^y/\sqrt{3})$	0.405	0.405	0.179
$R_{XZ}=f^y_{xz}/(f^y/\sqrt{3})$	0.405	0.405	0.179

gives the yielding rates used for each orthogonal direction and temperature level.

The mechanical properties used for the SG8 Radiata Pine can be found in the investigation developed by Frank Kang [14].

4. Numerical models

The finite element thermal model considers the hexahedron SOLID70 for the timber frame and also for the cladding gypsum. This element has eight nodes, each with one degree of freedom (temperature), uses linear interpolating functions and full Gauss integration $2 \times 2 \times 2$ [32]. The full-scale model also considers one additional interface finite element to account for the radiation inside the cavity and find this bulk temperature. The element SURF152 was applied to all internal surfaces from each of the eighteen cavity regions (wood and gypsum surfaces) from the full-scale model, overlaying the same nodes of the SOLID70 mesh, using an extra node for the radiation temperature in the cavity (bulk temperature). This element has four nodes plus this extra node, considers linear interpolating functions and full Gaus integration 2×2 [32].

The mesh is depicted in Figs. 6 and 7, for both scaled thermal models. The number of elements was determined through a convergence test of the solution.

For the structural analysis, the model considers the hexahedron SOLID185 finite element applied only to the timber frame. This element has eight nodes, each with three degrees of freedom (translations in each spatial direction UX, UY; UZ), uses linear interpolating functions and full Gauss integration $2 \times 2 \times 2$, with enhanced strain calculation [32]. The reduced scale model also includes an interface element COMBIN39 [32], used to simulate the lateral restrain effect of the simulated furnace frame usually used in the load-bearing fire tests. According to the standard EN1365-1 [12], the width of the specimen is less than the opening in the furnace frame, with a clearance between 25 (mm) and 50 (mm) from the lateral edges of the test specimen. This clearance only restrains the in-plane motion of the wall studs towards the frame, and should not offer any restrain in the opposite direction. This element behaves mainly under a compression load, following the characteristics of

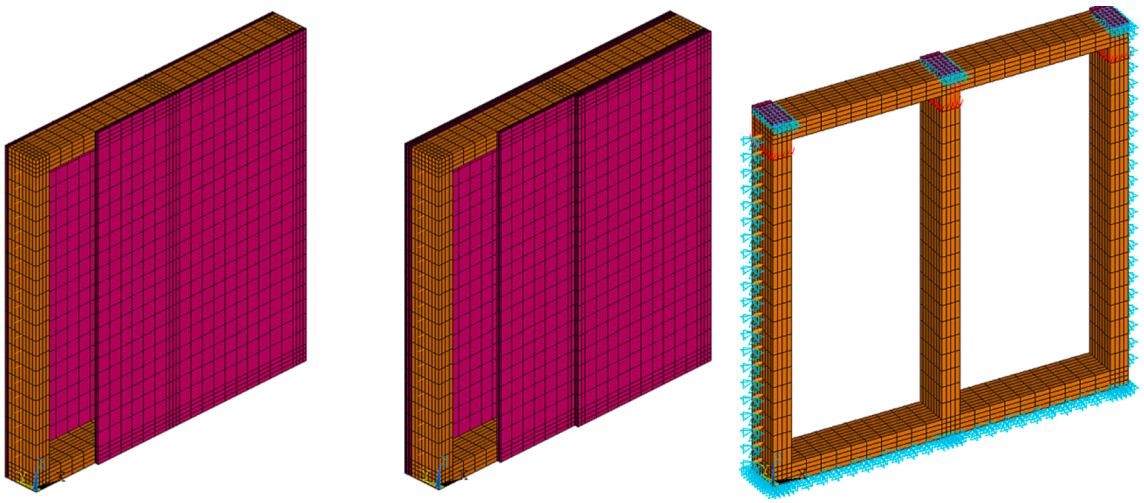

Fig. 6. 3D finite element mesh used for the reduced-scale model.

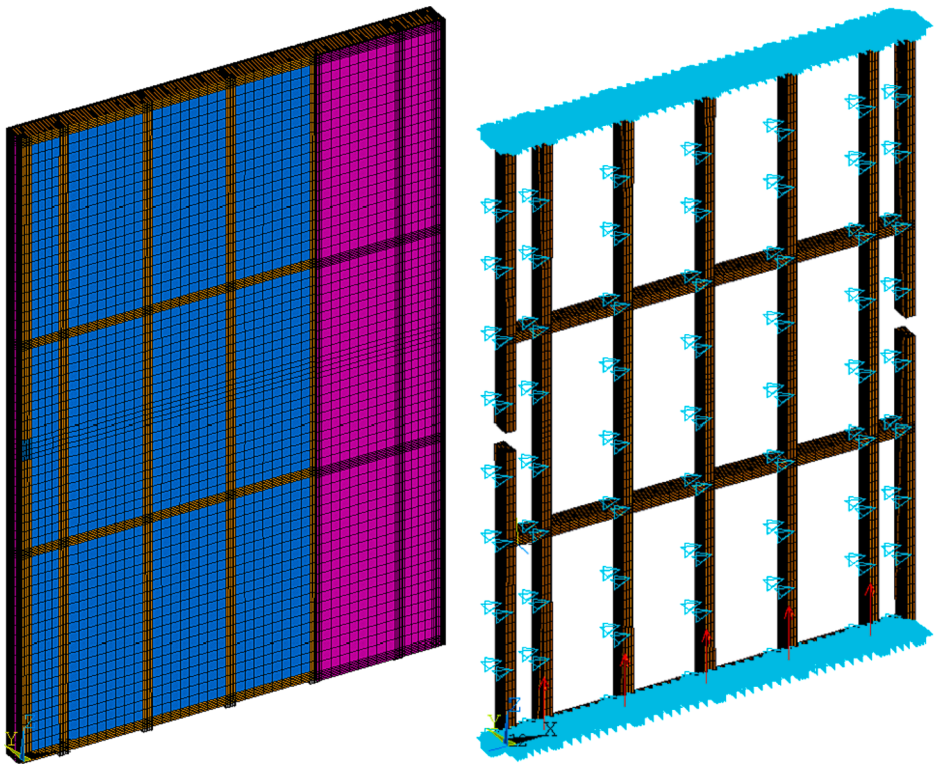

Fig. 7. 3D finite element mesh used for the full-scale model.

force–displacement depicted in Fig. 8. This element has not been used for the full-scale model, because the LTFW is included in the furnace volume with a clearance distance of 500 mm from the edges of the furnace frame.

The mechanical boundary conditions are also depicted in Figs. 6 and 7. Some additional in-plane restrains have been included in the full-scale model, by the screw effect in the connections of the gypsum plates to the timber frame.

The load-bearing capacity was determined for the reduced scale LTFW using the incremental load solution method. The maximum load-bearing was determined to be 151 (kN), regarding the shape of the load versus displacement of this structure defined for other fire ratings, considering the value for C = 2.6 (mm), [16]. The load-bearing capacity of the full-scale model was defined by the investigation of Frank Kang [14], and one load of 29 kN, using two hydraulic jacks, was applied in the LFTW to validate the numerical model.

A global imperfection, based on the maximum out of straightness equal to H/300 (H = height of the wall), was applied to the first instability mode to update the initial geometry of the reduced scale model. A smaller imperfection H/1000 value has been considered for the full-scale model.

Additional steel plates were used as an interface loading system in the area of each stud. This will help to avoid numerical problems related to the singularity of the nodal load applied for each bearing stud. These plates were modelled with 15 mm thickness, over the area of each bearing stud, using the finite element SHELL181. This element behaves in the linear elastic range, has four nodes, each with six degrees of freedom and uses linear interpolating functions for membrane and

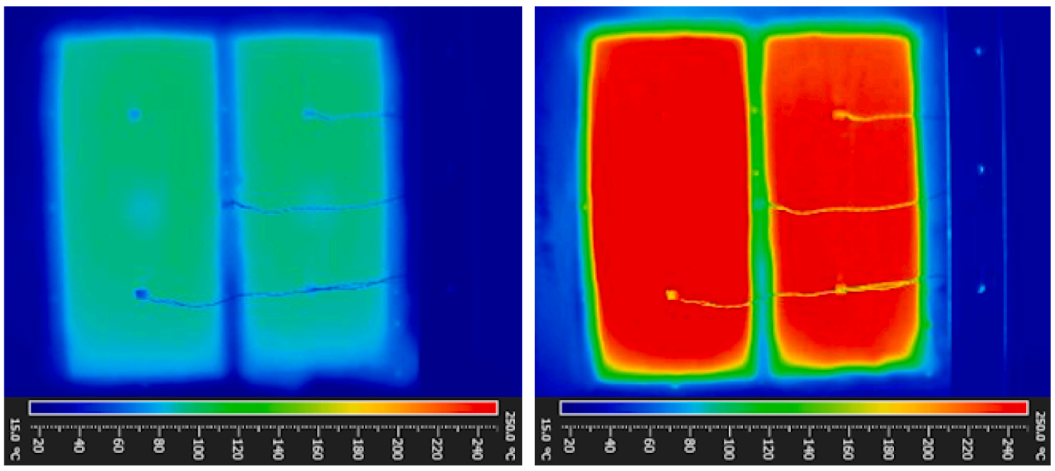

a) after 30 min. b) After 60 min.

Fig. 9. Infra Red temperature measurement on specimen 02. (For interpretation of the references to colour in this figure legend, the reader is referred to the web version of this article.)

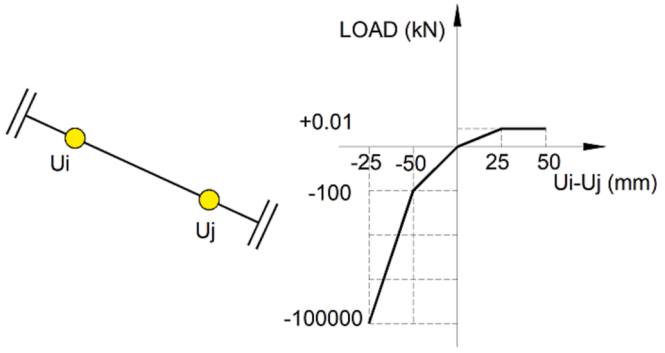

Fig. 8. Load-deflection curve for COMBIN39 finite element (not in true scale).

bending behaviour. The integration over the surface is performed with a 2x2 point Gauss rule [32].

5. Experimental tests

Two non load-bearing experimental tests were developed to find the ability to sustain the temperature of the LTFW (partition wall). These experimental tests were also used to validate the 3D thermal numerical model. The reduced scale specimens are presented in Table 4. The fire resistance was defined by the standard method, using copper Disk Thermocouples (DT) placed on the unexposed surface, allowing us to determine the maximum temperature (DT-T_{max}) and the average Temperature (DT-T_{ave}).

Non-standard measurement was also applied, using Infra Red thermal camera, allowing us to find the maximum (IR-T_{max}) and average temperature (IR-T_{ave}) in a wide region (almost unexposed area), see Fig. 9.

Temperature measurements were applied to several points in order to validate the numerical results and determine the ability to sustain the temperature on the unexposed side. According to the results presented in Table 4, the maximum difference between the numerical results (NUM) and the experimental results (EXP) is 14% and there is a perfect match for the T_{max} of the specimen 02 when compared to IR measurement. Fig. 10 depicts the position of control points. The central stud was drilled at half height with an array of thermocouples to measure the temperature of the cross section. The vertical distance between them is 20 mm and the depth is out of phase to avoid measuring interference. The thermocouples TT8 and TT9 are positioned 12.5 mm away from the most exposed edge side. Two additional Plate Thermocouples (PT) were applied in each cavity region. The experimental results will be presented in the next section for the validation of the numerical results, with RMS error calculation to determine the accuracy of the prediction model over time.

The main events during both tests are related to the initiation and progression of cracks, the fall-off of the gypsum plates and the ignition of the timber elements. Fig. 11 presents two photos from the exposed surface and two photos from the unexposed side, for different instants of time. Here one can see, from the inside of the furnace, both, the first crack and the fall off of the most exposed gypsum layer. On the other hand, from the ambient side, one can see, both, the unexposed surface after losing the insulation ability and the post fire after losing the integrity of LTFW (see the residual central stud).

Fig. 12 also presents three photos from the exposed side and one from the unexposed side. One can see the first vertical crack on the exposed gypsum layer, and the start of the ignition on the left stud. This figure also presents the unexposed surface after losing the ability to sustain the temperature and the residual timber frame after the end of the test. It is worth mentioning that specimen 02 with only one gypsum layer started to have flames inside the cavity at least at 36 min. At the same time ($t =$ 36 min), specimen 01 with 2 gypsum layers has not started the combustion process yet. The temperature inside the cavity is measured by the PT thermocouples (PT 1 and PT2). One can see that this temperature starts to rise after 40 min for specimen 01 and after 15 min for specimen 02. These values can be followed in the next section.

Table 4
Reduced-scale fire resistance specimens.

Specimen	Cladding (#xmm)	Studs and rails (mm)	Cavity fire scenario	$T_{0,ave}$	DT-T_{max} (min)	DT-T_{ave} (min)	IR-T_{max} (min)	IR-T_{ave} (min)	T_{max}-NUM (min)	T_{ave}-NUM (min)
01	2 × 12.5	100 × 50	01	21.0	94	98	91	95	104	102
02	1 × 12.5	100 × 50	02	17.9	52	53	47	50	47	49

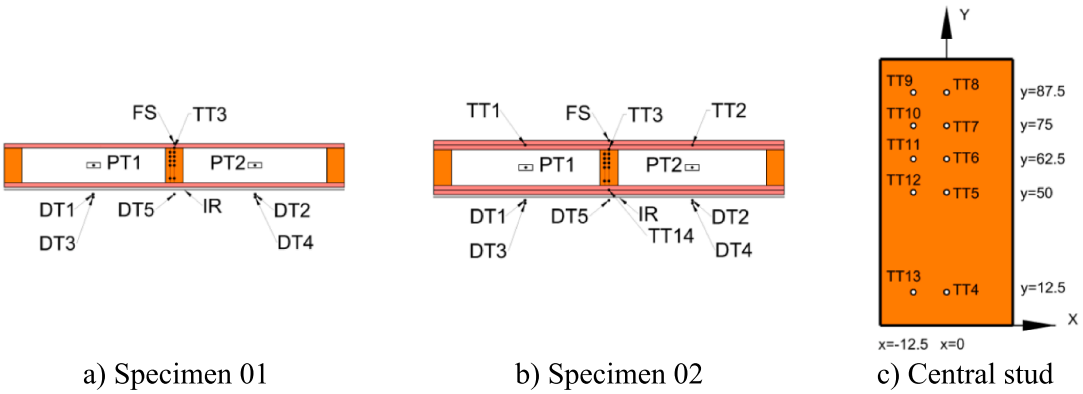

Fig. 10. Temperature measurements.

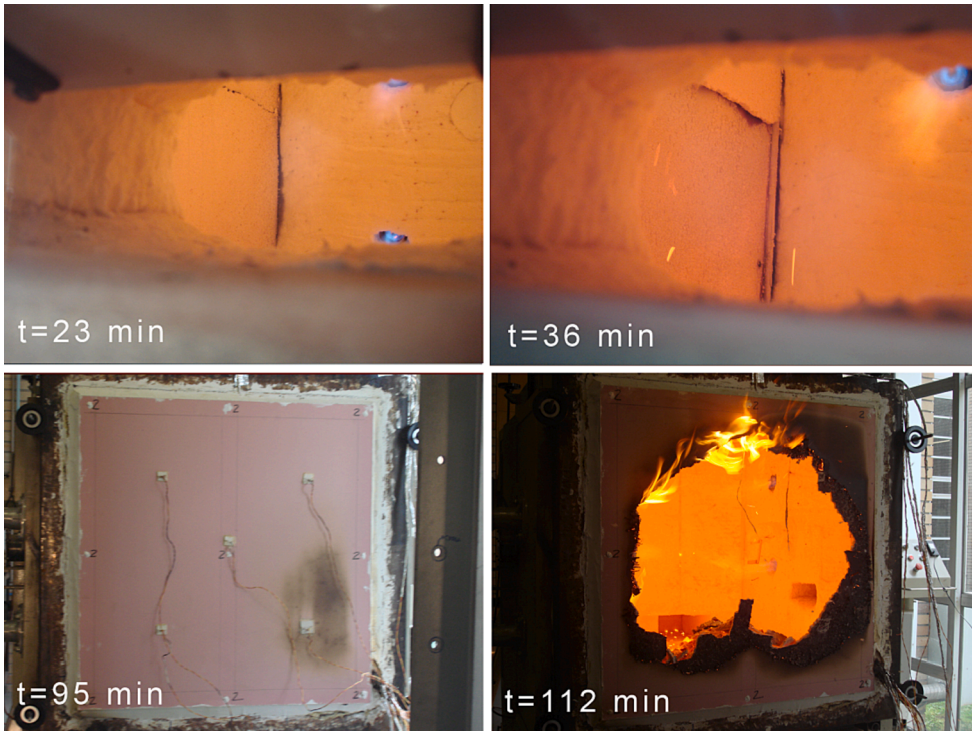

Fig. 11. Main events during the test of specimen 01: The first crack (t = 23 min). The fall-off from the most exposed gypsum layer (t = 36 min). The unexposed surface (t = 95 min). The post integrity failure (t = 112 min).

6. Validation of the numerical models

This section provides the comparison between the experimental results and the numerical results, for both the partition wall (reduced scale) and the load-bearing wall (full scale). Temperatures and displacements are going to be compared over time using the RMS error.

6.1. Comparison of the non load-bearing LFTW (reduced scale model)

Temperatures are going to be compared for certain positions on the wall and over the unexposed surface, where the ability to sustain the temperature allows the definition of the fire resistance by insulation. Specimen 01 has double gypsum plates, allowing for higher fire resistance. The numerical results are based on the less exposed nodal temperatures and superposed with experimental results, determined by DT and IR, see Fig. 13. The RMS error for T_{max} is 7.5 °C during the fire test of the specimen 01 and the RMS error for T_{ave} is 32.1 °C, both over a time window of 110 min, which is considered a very good approximation over time. The RMS error for the Specimen 02 increased for the T_{max} and decreased for the T_{ave}, being 56.8 °C and 17.3 °C, respectively and for a time window of 60 min, see Fig. 13.

Results were also compared for certain positions of the LFTW, especially for the fire side (FS) which represents the temperature of the most exposed gypsum, for the temperatures between both layers of gypsum (TT1 and TT2) and also for the position TT3, which represents the interface between the central stud and the gypsum plate, see Fig. 14. One can see that the temperatures measured in the central stud section (x = 0, TT4 …TT8, green colour) started to increase with a delay with respect to the temperatures measured near the cavity region (x = −12.5 mm, TT 9… TT13, blue colour). This is justified by the two direction heat flow, one coming by conduction through the gypsum layer to the central stud, entering through the narrow edge of the stud, and the other heat flow coming from the cavity region, by convection and radiation, entering through the wider edge of the stud.

The RMS error for specimen 01 was 21 °C, 93 °C and 108 °C for the positions FS, TT1/TT2 and TT3 respectively. The RMS error for

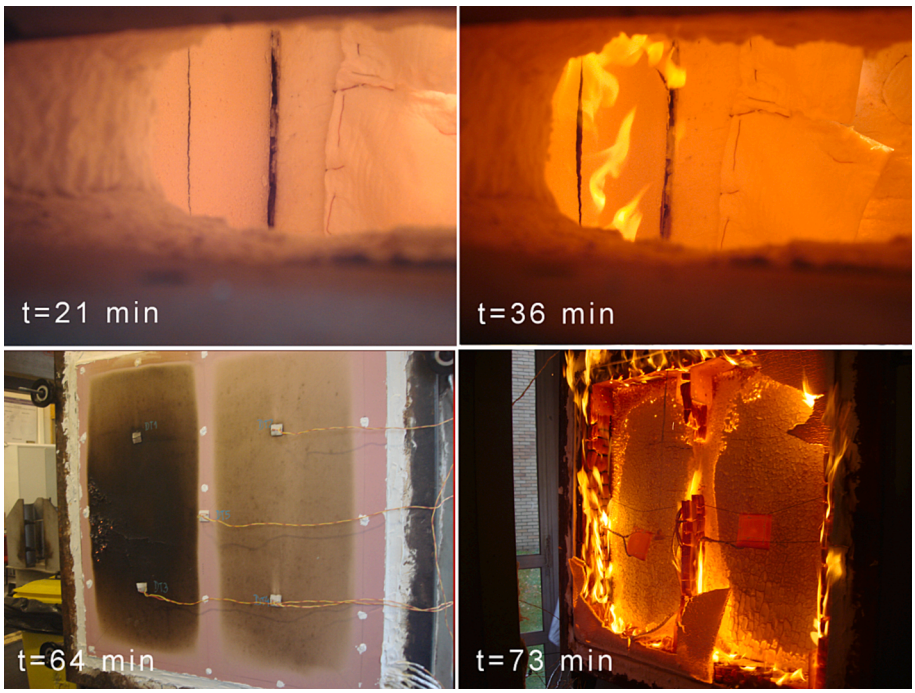

Fig. 12. Main events during the test of specimen 02: The first crack on the exposed gypsum layer (t = 21 min). The ignition of the left stud (t = 36 min). The unexposed surface after insulation failure (t = 64 min). The post integrity failure with the residual timber frame (t = 73 min).

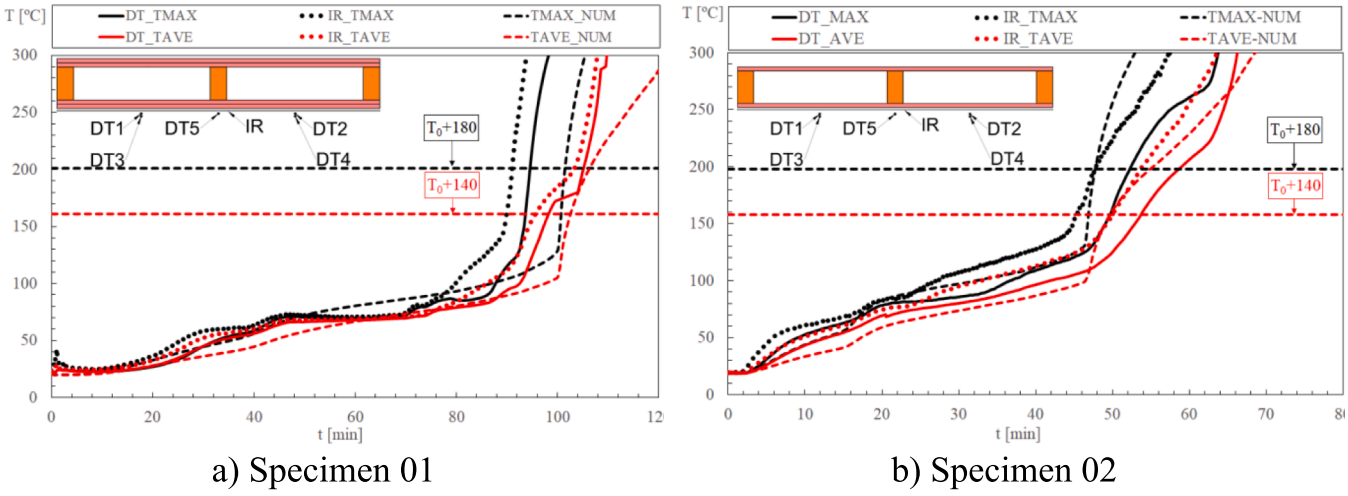

Fig. 13. Temperature on the unexposed surface of both specimens (reduced scale).

specimen 02 increased for the positions FS and TT3, being respectively 86 °C and 124 °C. These higher values may be justified by the use of thermo putty in excess for the FS thermocouple, and for the TT3 thermocouple, or by the combustion of the central stud that started at 30 min. These values reflect a good approximation, considering that, at any time after the first 10 min of any standard fire test, the temperature recorded by any thermocouple in the furnace shall not differ from the corresponding temperature of the standard temperature/time curve by more than 100 °C [23].

The 3D finite element model can also give a good approximation for the residual volume of the timber frame, as represented in Fig. 15, using the criterion of the 300 °C isothermal. The residual volume is presented for both specimens after 45, 50, 60 and 70 min. After 45 min there is not any reduction for specimen 01 but specimen 02 is already affected. After 50 min, specimen 01 starts to be affected while specimen 02 is more affected, including the central stud. After 60 min, the most exposed side and the surface near the cavity from specimen 01 present charred material, while the degradation of specimen 02 continues. Higher degradation is presented for 70 min of fire exposure. The residual frame of Specimen 01 is also depicted for 100 min of fire exposure.

The residual volume is always higher for the specimen 01 due to the higher number of gypsum layers. One can also compare the predicted residual frame with both photos in Figs. 11 and 12, which reflects a very good estimation.

6.2. Comparison of the load-bearing LTFW (full-scale model)

Temperatures and displacements are going to be compared for certain positions on the load-bearing wall, where the ability to sustain the load allows the definition of fire resistance by stability.

The temperature was compared in the central stud of the model for the positions P2 and P3, which are defined at 10 mm and 20 mm from

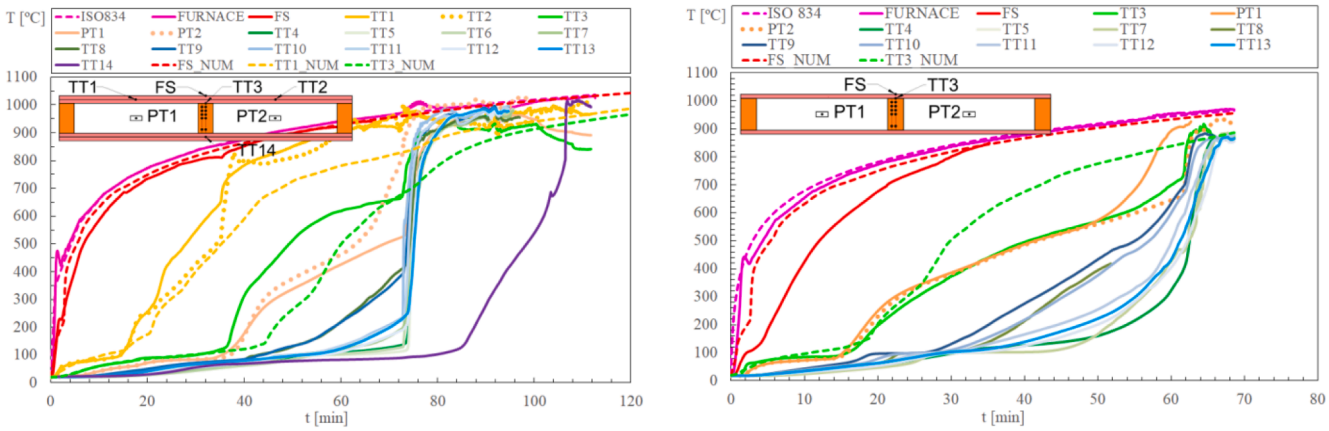

Fig. 14. Temperature in specific positions of the LTFW of both specimens (reduced scale).

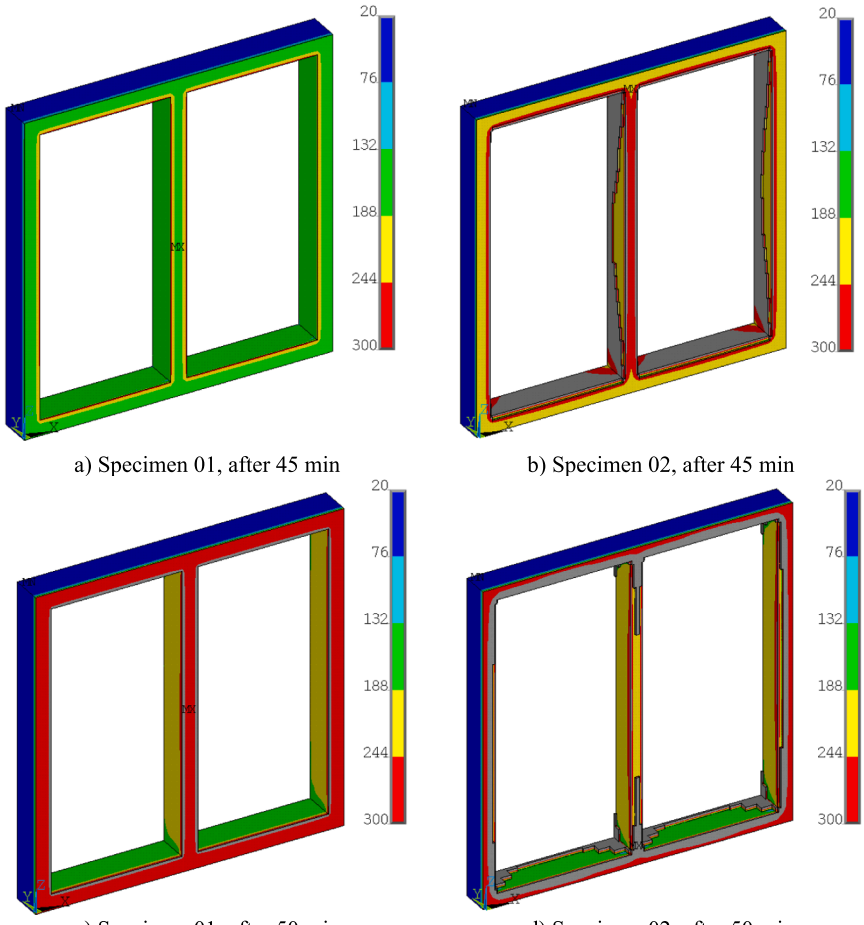

Fig. 15. Finite element results from thermal analysis of the reduced scale models for both specimens.

the most exposed edge of the stud, respectively. According to the experimental results, the numerical model presents a small delay for the increase of both temperatures, but even though, the difference is not big, see Fig. 16. The differences may be explained by the formation of cracks in the gypsum, the existence of gaps in the gypsum plates during the test, the fall down of parts of the gypsum plates, and the ignition and combustion of the timber frame. Besides these singular events, there should be some differences in material properties (model and real material behaviour), differences in the boundary conditions (temperature from furnace sides 1, 2 and 3) and the existence of convection heat transfer in the cavity region (not considered in the full scale model).

The vertical displacement fits very well with the experimental results, anticipating the structural failure by 2.5 min. The RMS error between the numerical result obtained for the central stud-S3 and both

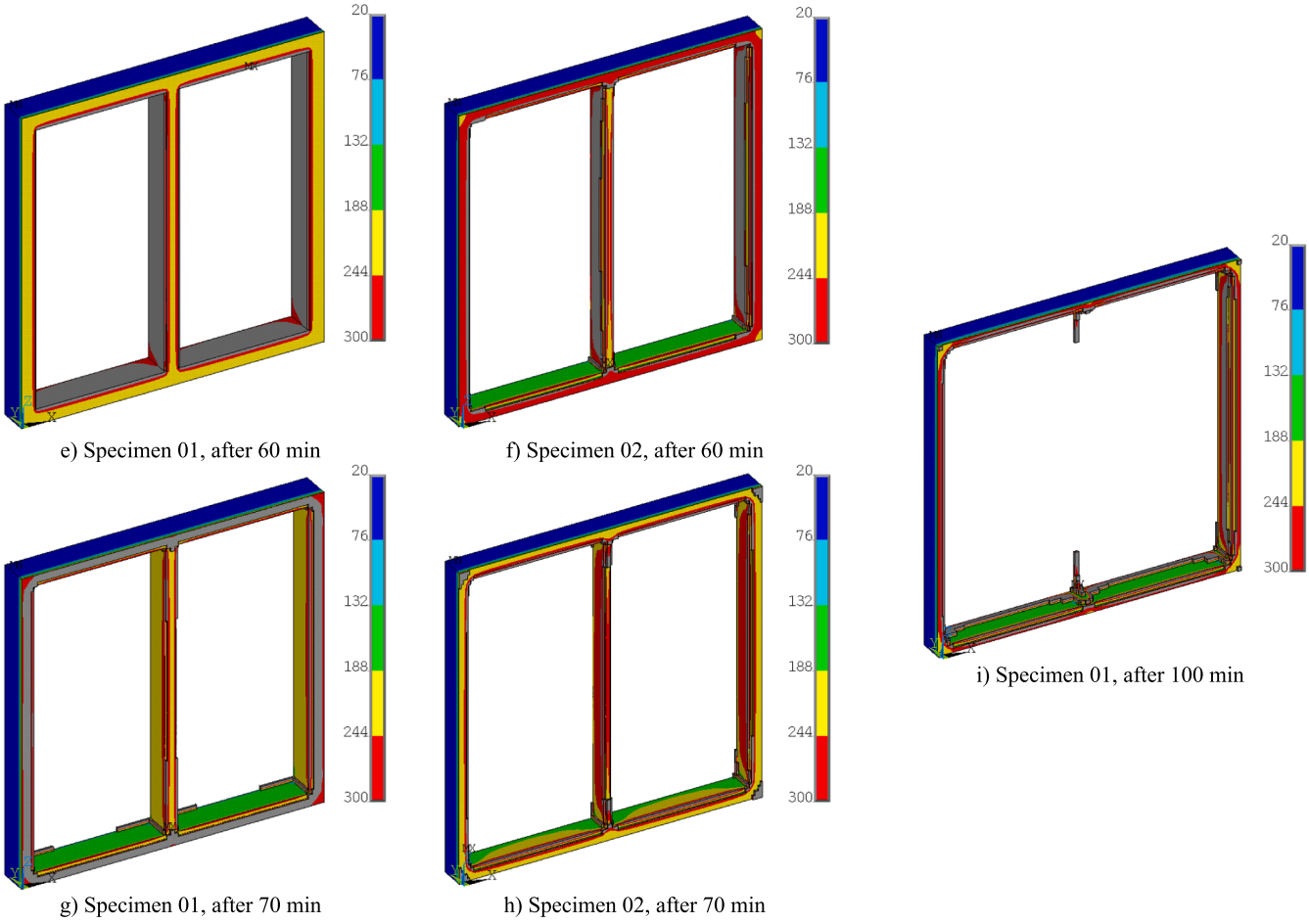

e) Specimen 01, after 60 min

f) Specimen 02, after 60 min

i) Specimen 01, after 100 min

g) Specimen 01, after 70 min

h) Specimen 02, after 70 min

Fig. 15. (*continued*).

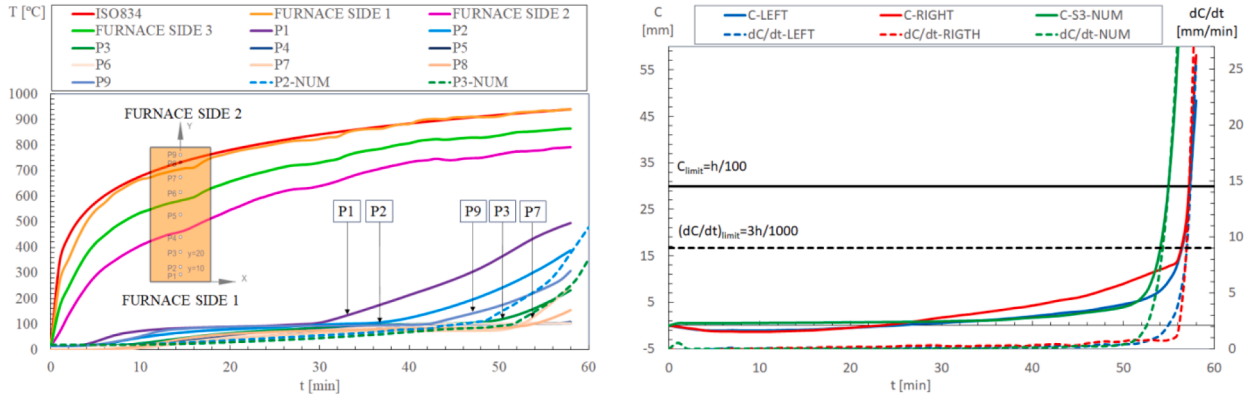

a) Results from thermal analysis

b) Results from thermo-mechanical analysis

Fig. 16. comparison of the results for the full-scale model.

experimental results (C-LEFT and C-RIGHT) are 0.8 and 2.5 mm, respectively, during the simulation and for the time window of the first 50 min. These values reflect the good approximation between the numerical and experimental results, considering that the criterion used to find the fire resistance is determined by the height of the wall (h) divided by 100. In this case, the critical displacement (contraction) would be 30 mm. Moreover, the measuring equipment shall meet the levels of precision of ±0,5 mm for the axial contraction [23].

The results can also be compared concerning the ability to sustain the load. The difference between the numerical results and the experimental criteria is below 5% for the contraction limit and 6% for the rate of contraction limit, see Table 5.

The 3D finite element model can give a good approximation for the residual volume of the timber frame, and also the deformed configuration, as represented in Fig. 17. The residual volume was determined using the criterion of the 300 °C isothermal. The deformed shape mode is in agreement with the experimental results developed by Frank kang [14].

Table 5
Comparison of the fire resistance.

Specimen	Cladding (#xmm)	Studs and rails (mm)	$T_{0,ave}$	Criterion	C-NUM min	C-LEFT min	C-RIGHT min	C-EXP Ave min	Diff. %
Full-scale	1 × 16	90 × 45	20	C_{lim} $(dC/dt)_{lim}$ Equilibrium	54.9 54.2 59.0	57.2 56.9	57.9 58.9	57.5 57.9	5 6

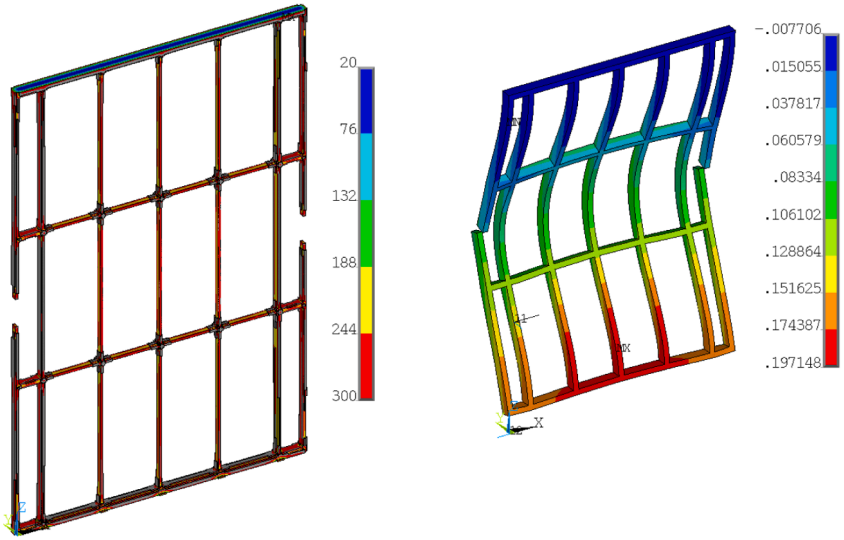

a) Residual timber frame with temperature b) Vertical displacement and deformed shape mode

Fig. 17. Numerical results for the full-scale model at 57.9 min.

6.3. *Parametric analysis for load-bearing reduced scale model*

This parametric study considers the effect of the load level, changing between 5% and 20% of the maximum load-bearing at room temperature. Also includes the effect of the protection level applied to the LTF, using one single layer of gypsum with 12.5 mm and two layers of the same thickness. Fig. 18 represents the vertical contraction of the timber structure with respect to time. The initial displacement (solid line) is due to the mechanical load, then the LTF reaches a plateau and after a certain period of time the displacement tends to increase very fast, reaching the displacement limit. This is the time when the LTF reaches a very big rate of displacement (dashed line). This figure also represents the rate of displacement and both limits for $C = 10$ (mm) and $dC/dt = 3$ (mm/min). The LTF structure is deformed and all simulated models attained the global bucking deformed shape mode, with studs moving in the direction of the outside of the furnace, due to the effect of load and charred layer, see Fig. 19.

The fire resistance of a double protected LTF is higher than the fire resistance of a single protected LTF, and both decrease with the load level. The fire resistance changes linearly with the load level. A new proposal is presented between the fire resistance t_{fi} and the load level μ, see Fig. 20.

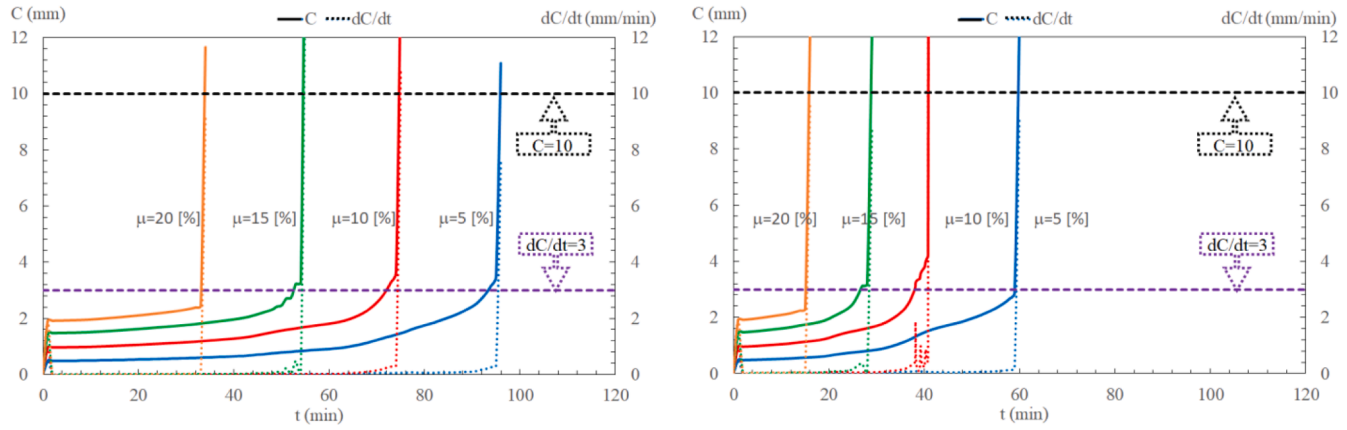

a) Specimen with double layer b) Specimen with single layer

Fig. 18. Numerical results for displacement over time: Parametric study.

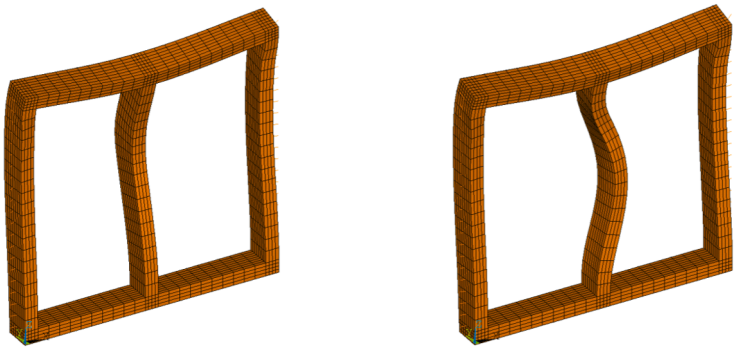

a) Specimen with double layer, with 5% load level, at 95 min.

b) Specimen with single layer, with 10% load level, at 40.7 min

Fig. 19. Numerical results for the defomed shape mode: Parametric study.

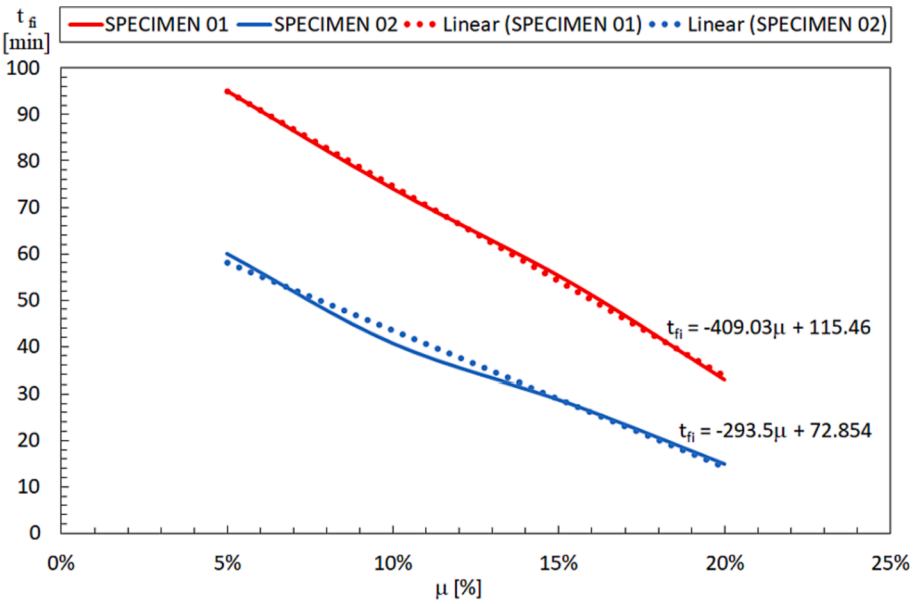

Fig. 20. New proposal for the fire resistance of LTFW when using single layer 1 × 12.5 mm gyspum and using double layer 2 × 12.5 mm.

7. Discussion of results

This investigation presents the numerical investigation about the effect of the load and protection level applied to the light timber frame walls. The numerical model is validated for temperature measurement using a reduced scale model, having developed two experimental tests for this purpose. The numerical model is also validated for displacement using a non standard fire test developed by Frank Kang [14], where the specimen was submitted to fire from both sides.

One of the most important steps is to model the thermal effect of LTFW with a void cavity as close as possible to reality. For this purpose, one should use the information of the bulk temperature developed in this region, in order to capture any opening crack, material degradation and the ignition of the timber frame. The bulk temperature can be measured during the experimental tests, which is the preferred method for validation of the numerical model, or determined by heat flow calculation, using appropriate interface elements to predict this cavity temperature.

The other important step is to model the thermo mechanical behaviour of the LTF without any finite element that should not be considered with the ability to sustain the load. This explains the removal of part of the model (gypsum finite elements) that were used during the previous simulation. Even though, the effect of this cladding system is partially included in this thermo-mechanical model, because the screws introduce a restrain effect in the horizontal direction. The reduced scale model also includes a different interface element to avoid any lateral deflection of the external studs into the direction of the furnace frame. The orthotropic behaviour with plasticity and Hill criterion should be used in order to predict the mechanical behaviour of the timber frame, using a local coordinate system to correctly align the material properties according to the three main directions.

The effect of the cladding system is of great importance, because the ability to sustain the load depends on the temperature history of the light timber frame. With two layers of gypsum plates, the fire resistance is higher and the model with one layer suffers a reduction of 46% on average.

The effect of the load level was also determined. The specimen with 2 layers of gypsum plates decreases the fire resistance faster than the gypsum with 1 layer. This effect is reflected in the new proposal formula, given by Eqs. (1) and (2).

Specimen 1

$$t_{fi} = -409.0 \times \mu + 115.4 \quad (1)$$

Specimen 2

$$t_{fi} = -293.5 \times \mu + 72.8 \quad (2)$$

8. Conclusions

The ability to sustain the temperature below a certain level on the unexposed side of the LTF wall (insulation criterion- I) is higher when using two gypsum layers. This ability is reduced by 50% when using one single layer of gypsum. The ability to sustain the load of the LTF (load-bearing criterion – R) is also higher in the case of the LTF wall protected by two gypsum layers. This ability is reduced by 46%, on average, when using only one gypsum layer. The timber frame is deformed under fire and all simulated models attained the global bucking instability mode, with studs moving to the outside of the furnace, due to the effect of load and charred layer. Some specimens also included flexural buckling with respect to the minor axis, for the last time increment of equilibrium, due to the inexistence of the in-plane restrain effect. The fire resistance of a double-layered protected LTF wall is higher than a single-layered LTF wall, and both decrease with the load level. The specimens with two layers of gypsum decrease their fire resistance faster than the specimens with one gypsum layer, with respect to the increase of the load level. The numerical criterion used to stop the simulation, in order to define the ability to sustain the load, is defined by the last stable equilibrium configuration. This configuration has always passed the time defined by the criteria used in the experimental standard EN1361-1 [23], regarding the critical maximum contraction displacement and rate of displacement. A new formula is also proposed to define this ability, based on the fire resistance and the load level.

CRediT authorship contribution statement

Paulo A.G. Piloto: Conceptualization, Methodology, Writing – original draft, Visualization, Investigation, Software, Validation. **Diego Vergara:** Investigation, Writing – review & editing.

Declaration of Competing Interest

The authors declare that they have no known competing financial interests or personal relationships that could have appeared to influence the work reported in this paper.

Data availability

Data will be made available on request.

Acknowledgements

Special thanks are due to Frank Kang for supplying the experimental results in full scale specimens and also to the company Winstone Wallboards Ltd, Australia.

References

[1] CEN. EN 13501-2: fire classification of construction products and building elements – Part 2: Classification using data from fire resistance tests, excluding ventilation services, CEN. Brussels: CEN; 2016.
[2] CEN. pr EN 1995-1.2, Eurocode 5: Design of timber structures – Part 1-2: General – structural fire design. CEN – European Committee for Standardization, Brussels; 2020.
[3] Mehaffey JR, Cuerrier P, Carisse G. A model for predicting heat transfer through gypsum-board/wood-stud walls exposed to fire. Fire Mater 1994;18(5):297–305. https://doi.org/10.1002/fam.810180505.
[4] Thomas GC, Buchanan AH, Carr AJ, Fleischmann CM, Moss PJ. Light timber-framed walls exposed to compartment fires. J Fire Prot Eng 1995;7(1):15–25. https://doi.org/10.1177/104239159500700102.
[5] Thomas GC. Fire resistance of light timber framed walls and floors. University of Canterbury; 1996. https://doi.org/10.26021/3544. PhD thesis.
[6] Takeda H, Mehaffey JR. WALL2D: a model for predicting heat transfer through wood-stud walls exposed to fire. Fire Mater 1998;22(4):133–40. https://doi.org/10.1002/(SICI)1099-1018(1998070)22:4<133::AID-FAM642>3.0.CO;2-L.
[7] Piloto PAG, Fonseca EMM. Timber framed walls lined with gypsum plates under fire. In: 7th international conference integrity-reliability-failure; 2020. p. 547–56.
[8] Young S. Structural modelling of plasterboard-clad, light timber framed walls in fire. Australia: PhD Victoria University Technology; 2000. https://vuir.vu.edu.au/id/eprint/15517.
[9] Clancy P. Advances in modelling heat transfer through wood framed walls in fire. Fire Mater 2001;25(6):241–54. https://doi.org/10.1002/fam.773.
[10] Young SA, Clancy P. Structural modelling of light-timber framed walls in fire. Fire Saf J 2001;36(3):241–68. https://doi.org/10.1016/S0379-7112(00)00053-9.
[11] Collier PCR, Buchanan AH. Fire resistance of lightweight timber framed walls. Fire Technol 2002;38(2):125–45. https://doi.org/10.1023/A:1014459216939.
[12] Clancy P. A parametric study on the time-to-failure of wood framed walls in fire. Fire Technol 2002;38(3):243–69. https://doi.org/10.1023/A:1019882131985.
[13] Thomas G. Modelling thermal performance of gypsum plasterboard-lined light timber frame walls using SAFIR and TASEF. Fire Mater 2010;34(8):385–406. https://doi.org/10.1002/fam.1026.
[14] (Frank) Kang H. The performance of timber-framed load-bearing gypsum plasterboard walls subjected to two-sided fire exposure. University of Canterbury; 2021.
[15] Piloto PAG, Rodríguez-del-Río S, Vergara D. Fire analysis of timber-framed walls lined with gypsum. Materials (Basel) 2022;15(3):741. https://doi.org/10.3390/ma15030741.
[16] Piloto PAG, Fonseca EMM. Load-bearing capacity of light timber frame walls under fire. Math Comput Sci 2022;16(1):1–16. https://doi.org/10.1007/s11786-022-00521-y.
[17] Rajakumar C, Rogers CR. The Lanczos algorithm applied to unsymmetric generalized eigenvalue problem. Int J Numer Methods Eng 1991;32(5):1009–26. https://doi.org/10.1002/nme.1620320506.
[18] Riks E. An incremental approach to the solution of snapping and buckling problems. Int J Solids Struct 1979;15(7):529–51. https://doi.org/10.1016/0020-7683(79)90081-7.
[19] Paulo Piloto, Khetata M, Gavilán A. Fire resistance tests of non-loadbearing LSF walls. In: TEST&E 2019 – 2nd conference on testing and experimentations in civil engineering – proceedings; 2019. p. 429–440. http://doi.org/10.5281/zenodo.3355354.
[20] Khetata SM, Piloto PAG, Gavilán ABR. Fire resistance of composite non-load-bearing light steel framing walls. J Fire Sci 2020;38(2):136–55. https://doi.org/10.1177/0734904119900931.
[21] CEN. EN 1991-1-2, Eurocode 1: Actions on structures – Part 1-2: General actions – Actions on structures exposed to fire. CEN-European Committee for Standardization. CEN-European Committee for Standardization, Brussels; 2002. p. 59.
[22] Bathe K-J, Ramm E, Wilson EL. Finite element formulations for large deformation dynamic analysis. Int J Numer Methods Eng 1975;9(2):353–86. https://doi.org/10.1002/nme.1620090207.
[23] CEN. EN 1363-1: fire resistance tests Part 1: General requirements. CEN-European Committee for Standardization, Brussels; 2020. p. 52.
[24] CEN. EN 1364-1: fire resistance tests for non-loadbearing elements. Part 1: Walls, CEN. Brussels: CEN; 2015.
[25] Iso. ISO834-1: fire-resistance tests – elements of building construction – Part 1: General requirements. Int Organ Standar 1999:25.
[26] AS 1530.4. Methods for fire tests on buildings materials, components and structures, Part. 4: Fire resistance tests of elements of building construction. Stand Aust; 2014.
[27] CEN. EN 1995-1-2, Eurocode 5: Design of timber structures - Part 1–2: General – structural fire design. CEN - European Committee for Standardization, Brussels; 2004. p. 1–69.
[28] Sultan MA. A model for predicting heat transfer through noninsulated unloaded steel-stud gypsum board wall assemblies exposed to fire. Fire Technol 1996;32(3):239–59. https://doi.org/10.1007/BF01040217.
[29] Holmberg S, Persson K, Petersson H. Nonlinear mechanical behaviour and analysis of wood and fibre materials. Comput Struct 1999;72(4):459–80. https://doi.org/10.1016/S0045-7949(98)00331-9.
[30] Rodney H, Soc R. A theory of the yielding and plastic flow of anisotropic metals. Proc R Soc London Ser A Math Phys Sci 1948;193(1033):281–97. https://doi.org/10.1098/rspa.1948.0045.
[31] Milhan TH. Numerical study on wooden beams subjected to high temperatures (in Portuguese). Instituto Politécnico de Bragança (MSc thesis); 2020.
[32] Ansys inc.. ANSYS® Academic Research, Release 2021 R2, Help System, Element reference. ANSYS Inc; 2021.